

## Flow Microwave Technology and Microreactors in Synthesis

Ian R. Baxendale,<sup>A,E</sup> Christian Hornung,<sup>B</sup> Steven V. Ley,<sup>C</sup>  
Juan de Mata Muñoz Molina,<sup>C</sup> and Anders Wikström<sup>D</sup>

<sup>A</sup>Department of Chemistry, University of Durham, South Road, Durham, DH1 3LE, UK.

<sup>B</sup>CSIRO Materials Science & Engineering, Clayton South, Vic. 3169, Australia.

<sup>C</sup>Department of Chemistry, University of Cambridge, Lensfield Road, Cambridge, CB2 1EW, UK.

<sup>D</sup>Biotage Sweden AB, Kungsgatan 76, SE-753 18 Uppsala, Sweden.

<sup>E</sup>Corresponding author. Email: [i.r.baxendale@durham.ac.uk](mailto:i.r.baxendale@durham.ac.uk)

A bespoke microwave reactor with a glass containment cell has been developed for performing continuous flow reactions under microwave heating. The prototype unit has been evaluated using a series of standard organic chemical transformations enabling scale-up of these chemical processes. As part of the development, a carbon-doped PTFE reactor insert was utilized to allow the heating of poorly absorbing reaction media, increasing the range of solvents and scope of reactions that can be performed in the device.

Manuscript received: 2 August 2012.

Manuscript accepted: 5 September 2012.

Published online: 8 October 2012.

### Introduction

The general strategies and synthetic protocols used to construct organic molecules have remained relatively unchanged over the last few decades despite the many conceptual and technological advances that have arisen. However, certain key enabling technologies, such as microwave heating<sup>[1]</sup> and flow-based chemical processing,<sup>[2]</sup> have seen rapid adoption and are greatly impacting on the synthetic routes used to prepare many of today's new chemical entities.<sup>[3]</sup> Furthermore, many existing syntheses have been re-examined and improved through the judicious application of modern chemical engineering principles and the integration of these new synthesis tools.<sup>[4]</sup>

We have previously demonstrated that coupling microwave irradiation and flow-based chemical processing can deliver synergy leading to improved throughput, superior yields, and higher-purity products.<sup>[5]</sup> However, much of our previous effort has been directed at methods of best utilizing commercially available microwave units through the development of bespoke microwave reactor inserts. Alternatively, in collaboration with one of the leading microwave vendors (Biotage AG), we wished to evaluate the potential for modification of a microwave unit and its suitability as a dedicated flow reactor platform for performing continuous flow-based microwave heating.

### Results and Discussion

Our prototype microwave unit was constructed from a reconfigured Biotage Initiator system (Fig. 1). The unit was removed from its outer case and the microwave irradiation chamber was inverted for easier access along with the fitting of several supplementary thermocouple temperature sensors to improve monitoring. As well as the thermocouple sensors sited at the inlet and outlet of the reactor, the internal IR probe of the microwave

unit can be used to monitor the surface temperature of the insert cell. Furthermore, a section of the irradiation containment chamber was removed to create a viewing window (Fig. 2b), enabling an IR camera to be used to record the heating process.

Situated within the microwave cavity, a simple straight glass cylinder capped with Teflon end-pieces was manufactured to function as the microwave reaction chamber (Fig. 2). The two Teflon seals were drilled to permit standard 1/4"-28 unified fine thread (UNF) microfluidic tubing connectors to be easily added for union with 1/16" perfluoroalkoxy (PFA) tubing, thus acting as direct inlet and outlet feed lines. The inside of these Teflon end-pieces have a reverse conical section, guiding the flow from the central inlet bore to the larger diameter of the glass cylinder. Consequently, the premixed reaction mixture driven using a standard HPLC pump enters the unit through the central inlet at the bottom and exits at the top (Fig. 2). The closing mechanism on the microwave cavity is used to securely hold the Teflon end-pieces in place, securing them within the glass tube. The system pressure is monitored using the pressure transducer on the HPLC pump with a maximum threshold of 20 bar set as a safety shutdown limit.

Using the service control software of the Biotage microwave, the wave guide can be manually adjusted to tune the microwave irradiation and regulate the power levels of the device. The real-time calibration data can be easily viewed on the digital display of the unit or recorded and exported from the system for additional processing in standard software such as Microsoft *Excel*. Instantaneous changes to the microwave parameters can easily be made in real time, facilitating reaction optimization and giving full system control over the heating process.

Before conducting any heating experiments, we first characterized the flow regime inside the empty reactor cavity. For this,

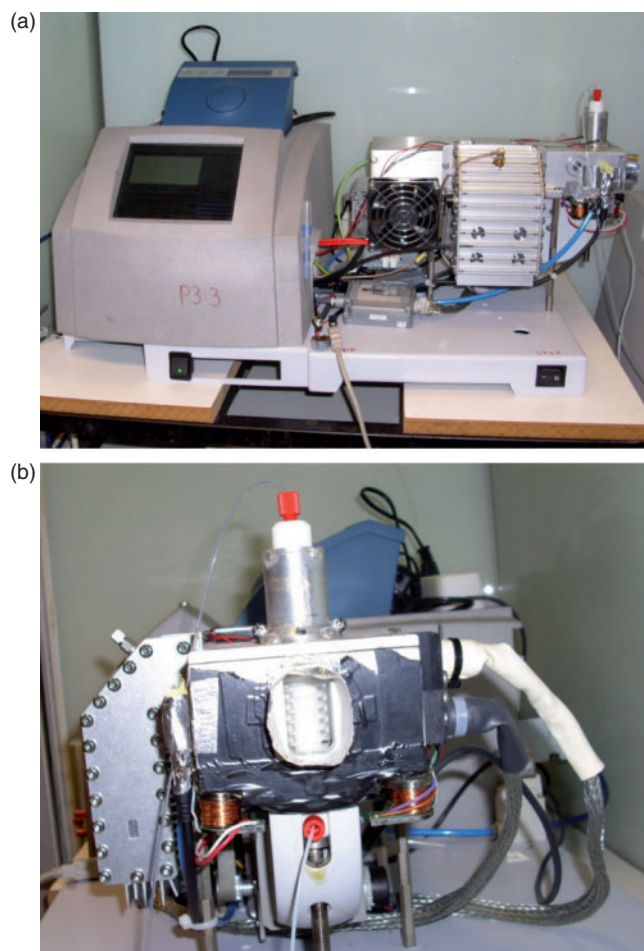


**Fig. 1.** (a) Microwave reactor front view. (b) Microwave reactor side view, with visualization port open showing the glass insert reactor.

a series of tracer dye experiments, using food colouring in aqueous and organic solvents, were undertaken. As can be seen from the photographs taken at steady-state conditions (Fig. 3, flow direction from bottom to top), clear channelling of the tracer dye through the chamber is observed at low flow rates ( $<1.3 \text{ mL min}^{-1}$ , Fig. 3a). At higher flow rates ( $3.5 \text{ mL min}^{-1}$ , Fig. 3b), a seemingly stagnant dome of dye forms at the centre of the flow chamber, and small ripples in the dye stream leading to it from the inlet can be observed. These ripples are generated by the pulsation of the HPLC pump and propagate through the reactor, which is operated at 100 psi using a back-pressure regulator (BPR) in-line after the reaction chamber. At higher flow rates ( $8 \text{ mL min}^{-1}$ , Fig. 3c), the dome disappears again and the ripples become more pronounced, forming small vortices either side of the centreline through the chamber. In any of these three examples, it is apparent that the flow generally channels through the centre of the cavity, with large dead volume surrounding this central flow path. The majority of the available reaction volume is therefore stagnant and unusable, and the flow is very inhomogeneous and greatly varies with flow rate. In order to improve this flow profile and use the available cavity as efficiently as possible for rapid microwave heating, we evaluated three different cavity-packing strategies.

Our first approach was to adopt the methodology previously used by Bagley and Mason<sup>[6]</sup> for the preparation of a series of heterocycles under continuous-flow microwave conditions,

where a column reactor was packed with either sand or glass beads (see also experimental section, Fig. 10, case 4). Although this gave in appearance a more even distribution of the dye through the flow reactor and increased the mean residence time (channelling was greatly reduced), there was also significant flow partitioning and the formation of dead zones. This could be easily seen by a simple flushing experiment (replacing dye solution with solvent) at  $0.25 \text{ mL min}^{-1}$ , which showed complete elution of the dye-saturated column took over 28 min for beads ( $500\text{--}600 \mu\text{m}$ ) and 39 min for sand ( $50\text{--}70 \text{ mesh}$ ). This compares with the theoretical residence times based on ideal plug flow of 13.7 min for beads (calculated void volume of 3.41 mL) and 11.1 min for sand (calculated void volume of 2.78 mL). Although potentially viable for processes involving long reaction times and stable reaction products, we felt this was far from an ideal scenario for all types of processing we wanted to investigate. Hence, we turned our attention to the construction of Teflon flow inserts that could be situated inside the tubular reactor cavity, acting as flow guides.

Two basic designs were manufactured: a simple recessed baffled core (with an alternating stepwise inclination) and a helical coil unit (Fig. 4a). Both inserts were machined from Teflon rods using standard machine cutting techniques (see the experimental section for technical drawings). These were then tested with dye injections to characterize their flow behaviour; photographs of tracer dye experiments using these two inserts are shown in Fig. 4b. Both units demonstrated greatly improved homogeneous flow characteristics and yielded a much narrower residence-time distribution. The baffled reactor insert gave a slightly larger internal (reaction) volume (baffled reactor, 3.2 mL; helical reactor, 2.5 mL) but also had more dead volume; consequently, for all further reactions, the helical coil was selected, which had the more uniform flow characteristics (see Fig. 4b).

## Reaction Testing

Microwave reactors have proved to be extremely valuable in organic synthesis but possess an inherent restriction due to the physical parameters of scaling up reactions. Restricted microwave penetration depths and power settings as defined by most commercial batch microwave reactors make direct scaling of reactor volumes difficult. Alternatively, conducting reactions in parallel using individually sealed batch reactor vials is possible but this is still suboptimal for larger-scale synthesis. Ideally, a continuous flow approach is best suited to scaling microwave reactions, as in any flow process, the required reactor volume is typically significantly smaller than that of a comparable batch reactor for the same product output. Therefore, we initially validated the system by conducting a series of trial scale-up experiments with the intention of preparing multigram quantities of material.

First, a Hantzsch reaction between 3-nitrobenzaldehyde and ethyl 3-oxobutanoate in the presence of ammonium acetate was performed, catalyzed by phenylboronic acid (5 mol-%) (Scheme 1).<sup>[7]</sup> The two stock solutions were combined and mixed using a 2-mL baffled mixing chip<sup>[8]</sup> before entering the microwave heating zone. Inside the microwave cavity, the reaction mixture was heated at  $115^\circ\text{C}$  with a flow rate of  $0.1 \text{ mL min}^{-1}$  per feed channel ( $0.2 \text{ mL min}^{-1}$  combined flow rate through the microwave reactor), giving a residence time of 12.5 min with a 100-psi BPR used to maintain a positive system pressure. The output stream was collected and approximately

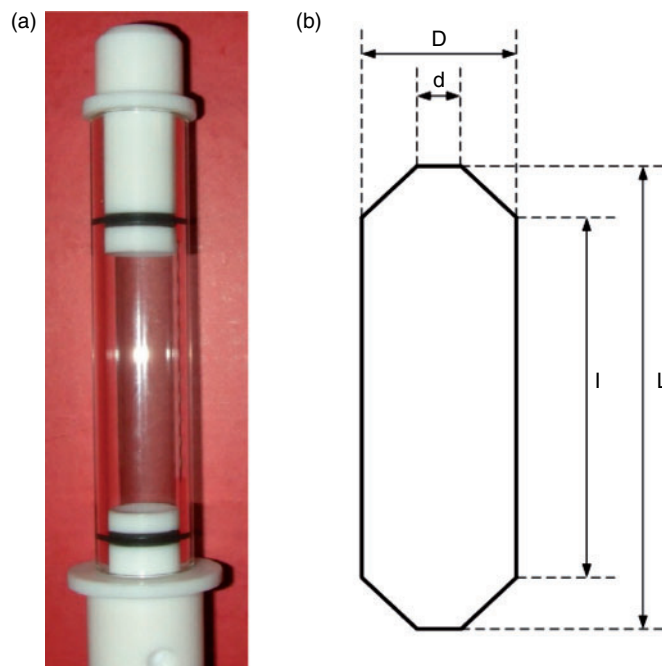


**Fig. 2.** (a) Tubular, flow-through microwave reaction chamber. The off-centre lateral alignment of the Teflon caps positions the clear glass section in the microwave irradiation zone within the cavity. (b) The inner diameter of the glass cylinder  $D = 15.0$  mm. The inlet and outlet bores at top and bottom have a diameter  $d = 1.9$  mm. The distance between them  $L = 59.0$  mm, and the length of the cylindrical section of the reactor cavity  $l = 53.8$  mm. Internal volume = 8.54 mL.

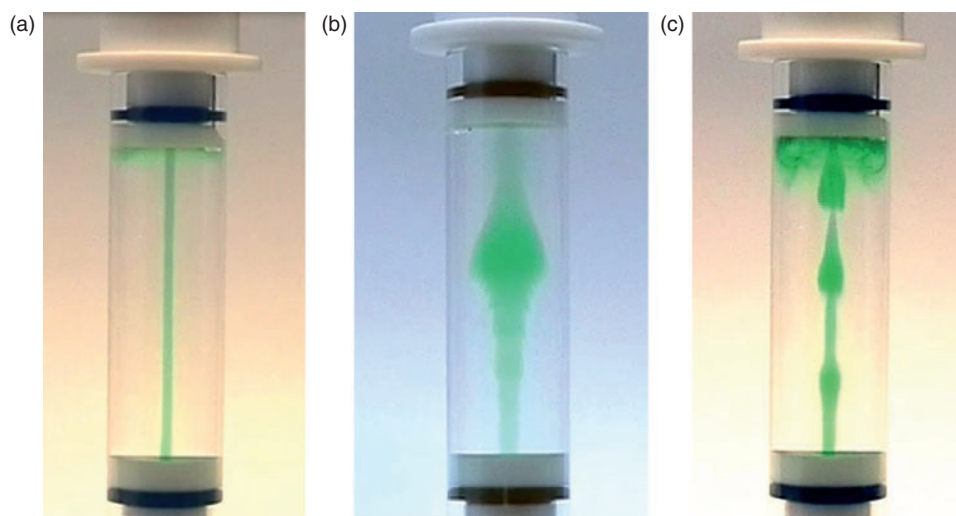


**Fig. 3.** Microwave reactor flow chamber. Tracer dye flow rates: (a) 1.3; (b) 3.5; and (c) 8 mL min<sup>-1</sup>. Flow direction: from bottom to top.

half of the ethanol solvent was evaporated under reduced pressure. The resultant solution was then left to stand at 5°C for 24 h to crystallize (no additional reaction was seen during this stage as identified by liquid chromatography-mass spectroscopy (LC-MS)). The solid material was filtered and dried under high vacuum to yield the dihydropyridine in 81 % isolated yield. The reactor was successfully run for 48 h at steady state (22-W constant power), processing 576 mL of reaction solution, equating to 349 g of isolated product. Periodically sampling the reactor throughout this run showed excellent reaction consistency ( $\pm 1.2$  % as determined by <sup>1</sup>H NMR analysis).

The second reaction we investigated was a palladium-catalyzed Suzuki cross-coupling, which had proved problematic in batch under standard thermal heating owing to the rapid formation of palladium black. This was especially troublesome when increasing the scale of the reaction (>10 g substrate) as the prolonged heating (reflux, 3.5 h) necessary to drive larger-scale reactions to completion also resulted in catalyst deactivation, requiring the addition of further portions of catalyst and ligand to ensure complete conversion (on average 5–8 mol-% catalyst loading was required). We anticipated that a more focussed heating sequence with a short residence time could help prevent

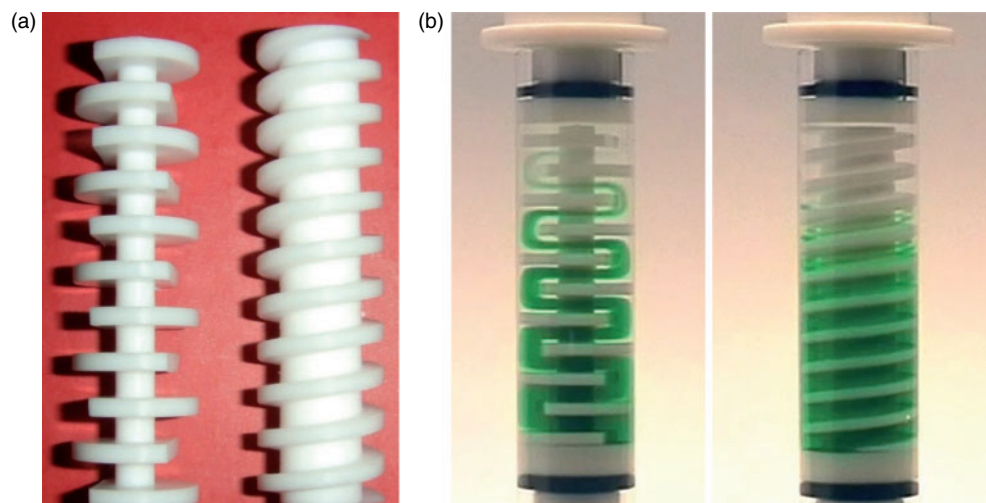
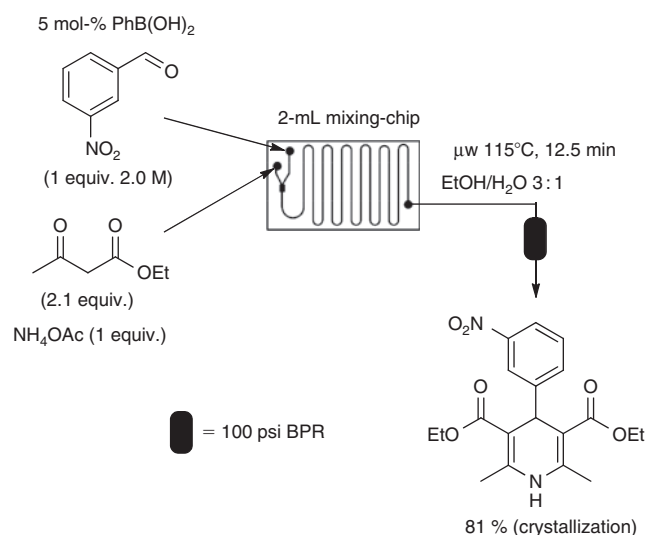
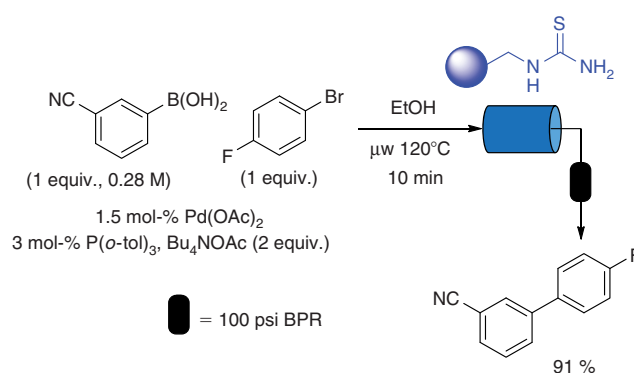


Fig. 4. Microwave reactor flow tube insert. (a) Teflon inserts. (b) Dye flow injections.



Scheme 1. Hantzsch condensation reaction performed under microwave flow conditions.

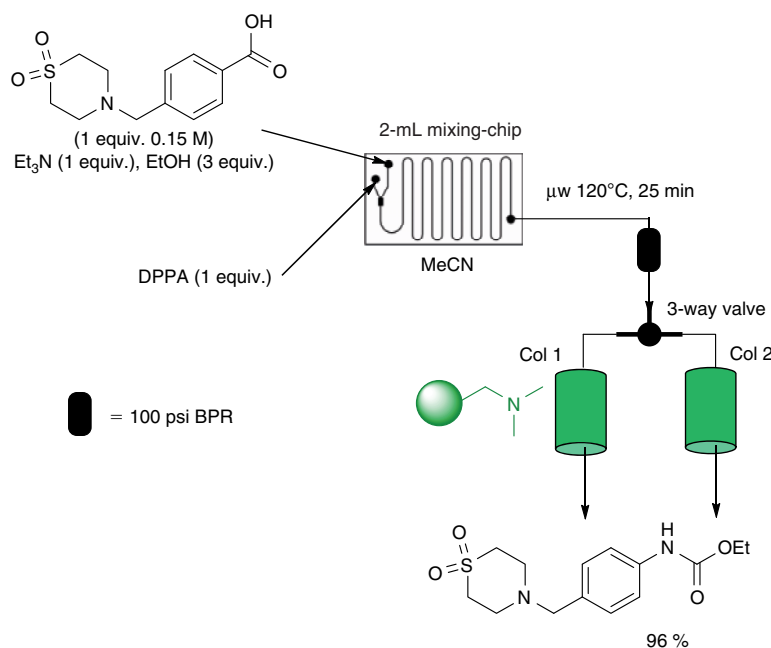
palladium aggregation and premature deactivation of the catalyst. Based on a rapid screen of batch microwave reactions, we were pleased to also determine that a lower quantity of palladium catalyst, amounting to only 1.5 mol-% of palladium, could be applied at elevated temperatures. Consequently, a homogeneous solution of the substrates, catalyst and base were prepared in EtOH (degassed by nitrogen purging) and pumped through the microwave reactor, which was maintained at 120°C at a flow rate of 0.25 mL min<sup>-1</sup>, equating to a residence time of only 10 min (Scheme 2). The exiting solution was then directed through a glass column packed with QP-TU (Quadrapure scavenger), a thiourea metal scavenger. The entire output was then collected for 28 h (420 mL throughput), the solvent then removed under reduced pressure and the residue taken up in EtOAc (250 mL) and extracted with saturated aqueous sodium hydrogen carbonate solution, 1 M aqueous potassium phosphate, dried over MgSO<sub>4</sub>, and finally, the EtOAc solvent removed. This gave a high-quality crude product (21.2 g, 91%) contaminated with only trace impurities of the tri(*o*-tolyl)phosphine (P(*o*-tol)<sub>3</sub>) ligand.<sup>[5b]</sup>



Scheme 2. Suzuki coupling process under flow microwave conditions.

Next, we investigated the formation of a carbamate adduct through a thermal Curtius rearrangement of a carboxylic acid promoted by diphenylphosphorylazide (DPPA) (Scheme 3).<sup>[9]</sup> This reaction has found general use as an effective processing tool for generating versatile and novel protected amine building blocks from their chemically diametric carboxylic acids, a reaction of significant interest to both the pharmaceutical and agrochemical industries.

Once again, a baffled mixing chip was used to ensure a homogeneous solution was produced from the two input streams before the material passed into the microwave reactor. A low flow rate equating to only 50 μL min<sup>-1</sup> per channel was used to deliver the starting materials, enabling a residence time within the cavity of 25 min. At the elevated temperature of 120°C used, the substrate underwent smooth rearrangement to the isocyanate, which was directly trapped in situ with the ethanolic nucleophile furnishing the carbamate in essentially quantitative conversion. Sampling the flow stream before the scavenging process showed only trace quantities of the starting carboxylic acid were present, and subject to the use of freshly distilled solvents, no urea dimers were detectable. The reaction was therefore run continuously over the course of 3 days (60 h, 360 mL). The only manual intervention needed was to switch an in-line three-way valve at the midpoint of the run (30 h) to change the scavenging cartridge. After flushing each of the two cartridges with MeCN at a higher flow rate of 3 mL min<sup>-1</sup>



**Scheme 3.** A Curtius rearrangement reaction under flow microwave conditions.

(30 min) to ensure complete elution of the product, followed by evaporation of the solvent (and  $\text{Et}_3\text{N}$ ), pure rearranged Curtius adduct (16.2 g, 96%) was isolated.

A further aspect of interest was that the constant generation of nitrogen gas from the Curtius rearrangement process was easily handled under the continuous flow conditions, preventing pressure build-up in the system. The nitrogen remained in solution owing to the presence of a 100 psi BPR; out-gassing occurred inside the scavenging cartridges but did not noticeably affect the efficiency of the sequestering process.

The Pechmann reaction has received significant interest in the literature with respect to microwave-assisted synthesis.<sup>[10]</sup> Although many of the reported preparations indicate the benefit of applying solvent-free conditions, an additional number identify rate enhancements and higher yields based on the rapid heating profiles achievable in a microwave reactor. Our view of these results is that much of this improvement can be directly linked to the lower stoichiometry of 1,3-dicarbonyl that can be used under the flash-heating conditions, especially when scaling up the reaction. During the reaction sequence, water is generated as part of the condensation mechanism, which in larger-scale reactions using long heating cycles can lead to hydrolysis and subsequent decarboxylation of the 1,3-dicarbonyl starting material. The resulting newly formed carbonyl by-product is a likely source of many additional adducts and contamination. Consequently, we were interested in the effect of applying rapid heating cycles achievable using our flow-through microwave chamber.

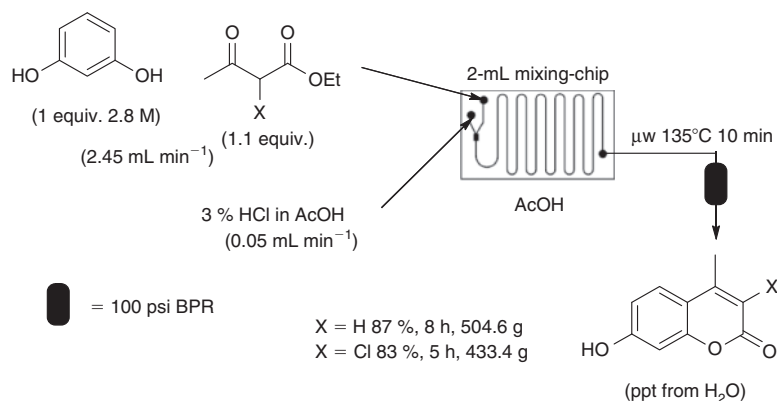
We therefore prepared a 3.8 M stock solution of resorcinol and the corresponding 1,3-dicarbonyl in acetic acid (AcOH), which was pumped into a 2-mL glass mixing chip that was heat-insulated with woven glass wool lagging. A second flow stream containing 3% HCl in AcOH (v/v) was injected into the main flow stream, generating a rapidly initiated exotherm (the chip temperature was 85°C under steady-state operation as determined by surface IR measurements). In-line sampling at the exit of the mixing chip showed that conversion to the desired product had occurred, amounting to ~53%. The reaction stream was

immediately directed into the flow microwave reactor where the temperature was rapidly raised to 135°C and the material was processed with a residence time of 10 min. The output flow was then directed into a vigorously stirred solution of water, which immediately precipitated the product as an off-white-cream solid. Filtration of the suspension and drying of the solid under vacuum over phosphorus pentoxide allowed isolation of the desired products in high yield (Scheme 4).

### Modification of the Reactor Insert for More Effective Heating

Having successfully demonstrated the use of the reactor on a series of trial reactions, we wished to investigate its utility for solvent systems that typically exhibit low absorbance of microwave irradiation. For example, synthetically useful solvents such as benzene, toluene or carbon tetrachloride couple weakly with the microwave field and consequently are difficult to heat, requiring long initial irradiation periods in order to achieve higher temperatures and then a constant high-power input to maintain the specified temperature. One classical way of circumventing this issue is to dope the reaction solvent with a strongly coupling heat-transfer component such as an ionic liquid.<sup>[11]</sup> However, this adds its own problems of workup and separation. We envisaged it should be possible to machine an alternative insert for our glass reactor casing made of a strongly absorbing material such as Si/C or carbon-mixed PTFE (Weflon<sup>TM</sup>).<sup>[1b,12]</sup> This would allow the microwave irradiation to couple directly with the internal structure of the reactor and convectively heat the solution as it flowed through. We therefore tooled a carbon-impregnated PTFE (C/PTFE) spiral reactor insert as a replacement for the previously employed Teflon unit (Fig. 5).

To test the enhanced heat-transfer capability of the reactor, we appraised it first in the radical allylation of an iodolactone (Scheme 5).<sup>[13]</sup> For this reaction, we selected carbon tetrachloride as the system solvent. The compatibility of  $\text{CCl}_4$  with the proposed radical chemistry and, importantly for a proof of



**Scheme 4.** Microwave-assisted Pechmann condensation reaction.



**Fig. 5.** Carbon impregnated PTFE (C/PTFE) microwave reactor insert.

concept, its lack of direct coupling with the microwave irradiation made it an ideal choice.

By using a very low flow rate of  $25 \mu\text{L min}^{-1}$  delivered by a Gilson 402 dual-piston syringe pump running in continuous mode (1 and 2.5 mL left and right syringes), we were able to achieve a residence time of  $\sim 100$  min, necessary for full conversion. To simplify this reaction, all the reagent inputs were premixed and the solution fed directly into the reactor, which was held at  $100^\circ\text{C}$  (100 psi BPR at exit). To further aid workup of the reaction, the reactor output was directed through a cartridge of QP-TU followed by a corresponding cartridge of QP-SA (Quadrature sulfonic acid), which made the subsequent chromatography separation step considerably easier (Fig. 6). Under these conditions, complete consumption of the iodo starting material was observed, yielding the desired product<sup>[14]</sup> in a respectable 78% yield accompanied by 12% of the formal elimination by-product.<sup>[15]</sup> The use of a lower reaction temperature or shorter residence time yielded incomplete conversion, which is also in accordance with the expected half-life and thus activity of the radical initiator 2,2'-azobis(2-methylpropionitrile) (AIBN).<sup>[16]</sup>

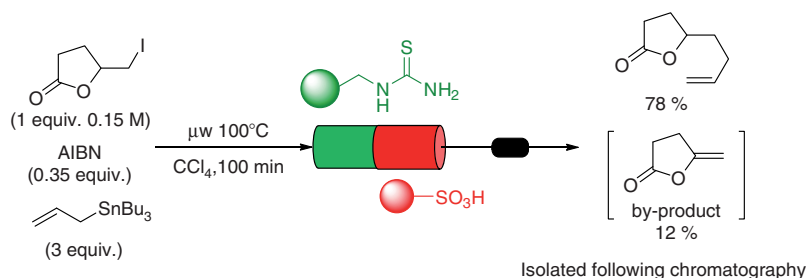
Of further interest was the rapid and linear heating profile that was observed when starting up the reactor, requiring only

48 s to reach the required  $100^\circ\text{C}$ . It should, however, be noted that this was also accompanied by a  $14^\circ\text{C}$  overshoot in the specified temperature before stabilized heating was achieved (16-W constant power). This highlighted a concern with regards to the extent of the temperature gradient extending from the C/PTFE core to the outer surface of the reactor where the temperature measurement was recorded by the IR probe. This non-homogeneity as seen in reverse when compared with classical oil-bath heating could result in a significant temperature gradient. We initially attempted to address this issue using an IR camera to quantify the radial heat distribution emanating from the core. Unfortunately, the finned and elongated spiral designs used to construct the core inserts created a lot of heat distortion, meaning the results were unclear. Our most consistent estimates based on IR measurements gave an  $\sim 6\text{--}9^\circ\text{C}$  difference between the core and the external reactor face. In fact, considering the same internal volume and large surface area of the insert core, it would be expected that heat transfer from the insert to the fluid was extremely efficient.

We therefore searched for a literature reaction that was known to be highly temperature-sensitive. Sarko et al. at Boehringer Ingelheim had used a 5-aminopyrazole-forming reaction to determine temperature differences across the various positions in a PTFE 96-well plate when heated under microwave irradiation in a CEM Mars 5 system.<sup>[17]</sup> The reaction (Scheme 6) was reported to display high temperature sensitivity, with temperatures exceeding  $120^\circ\text{C}$  giving decomposition of the starting materials whereas temperatures below  $80^\circ\text{C}$  failed to yield any product. The optimal conditions were determined to be  $110^\circ\text{C}$  and 5-min reaction time.

To standardize the reaction with our apparatus, we first performed the same transformation in a sealed batch microwave vial (2.5 mL, 0.25 M) using a standard Biotage Initiator system. Applying the previously optimized conditions, the reaction proceeded well, furnishing an 82% yield of the desired product. By comparison, attempting to run the reaction at  $80^\circ\text{C}$  gave only 6% conversion. However, we found the use of higher temperatures to be less significant than previously reported,<sup>[17]</sup> although yields did appreciably fall off at  $>140^\circ\text{C}$ , with an increase in the amount of decomposition seen (Fig. 7, blue curve).

We next ran the reaction under continuous-flow conditions with a flow rate of  $0.5 \text{ mL min}^{-1}$ , progressing through a series of incremental temperature changes. The temperature was increased in  $10^\circ\text{C}$  stages and the reactor allowed to equilibrate over a 10-min hold time (equating to  $2 \times$  mean residence time, processed volume = 5 mL), attaining steady-state operation.



**Scheme 5.** Radical allylation chemistry conducted using microwave irradiation.

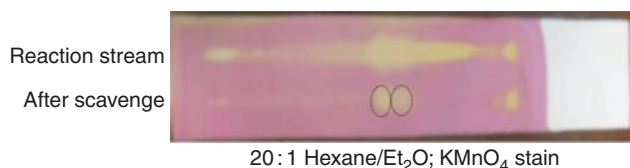
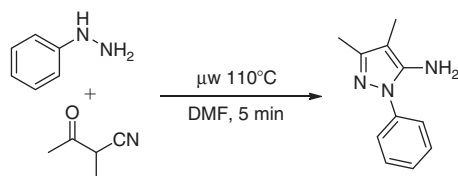


**Fig. 6.** Chromatogram run from left to right (top spot, by-product; lower spot, desired product).



**Scheme 6.** Temperature-dependent 5-aminopyrazole-forming reaction explored by Boehringer Ingelheim.

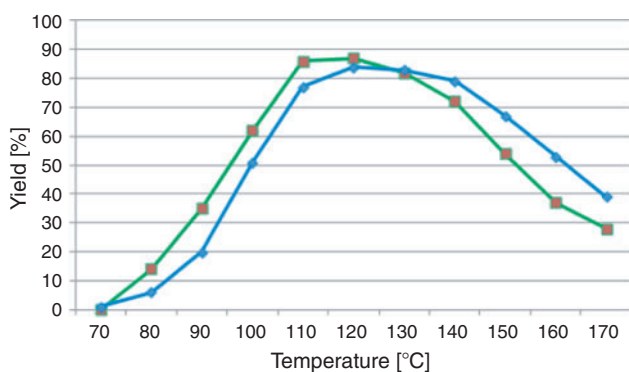
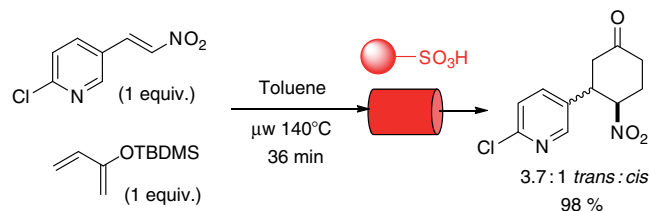


**Fig. 7.** Plot of isolated yield against temperature for the 5-aminopyrazole reaction depicted in Scheme 6. Blue curve, batch experiments; green curve, flow process.

An aliquot relating to one reactor volume (5-min processing time =  $1 \times$  mean residence time, processed volume = 2.5 mL) was then collected and analysed (Fig. 7, green curve) before raising the temperature again.

As can be seen from the plot, the lower temperature points (80–110°C) indicate a proportionally greater extent of reaction conversion in the flow system. Interestingly, this same trend is repeated when considering the extent of decomposition that occurs in the higher temperature ranges. Therefore, in conclusion, it would seem that the faster kinetics are in accordance with an increase in internal reactor temperature, as seen by the offset in the overlays. This being the case, it should be possible to



**Scheme 7.** Synthesis of the epibatidine cyclohexanone precursor under microwave heating. TBDMS: *tert*-butyldimethylsilyl.

validate this against a secondary parameter, namely system pressure (increased internal pressure of a heated solvent).

As DMF is a high-boiling-point solvent prone to degradation under microwave heating, we exchanged the reactor solvent for *n*-hexane (bp 69°C, low microwave absorbing  $\epsilon' = 1.9$ ,  $\delta = 0.20$ ,  $\epsilon'' = 0.038$ ).<sup>[17]</sup> For this experiment, we sealed the output of the reactor with a union connected directly to an electronic pressure sensor. The input port was also sealed with a simple blank 1/4"-28 UNF screw fitting. Raising the temperature of the sealed reactor to 70°C (monitored by the IR detector on the face of the reactor) gave a pressure reading of 1.23 bar (calculated to be equivalent to  $\sim 75^\circ\text{C}$  based on the pressure). We then steadily raised the temperature and recorded the corresponding pressure drop up to 140°C (7.23 bar, which would correspond to a reverse calculated temperature based on pressure of 146°C). These data confirm that there is indeed a temperature gradient, which must be localized very close to the core of the reactor but dissipates rapidly, giving a generally lower bulk temperature reading at the surface. This bulk variation based on the pressure change is  $\sim 6^\circ\text{C}$  from that recorded by the IR probe. This to us seemed a reasonable value considering the design of the apparatus and the inherent accuracy of measuring an internal temperature with a surface-focussed IR temperature probe. We were therefore confident to proceed with the testing, acknowledging the small temperature variation involved with this prototype unit.

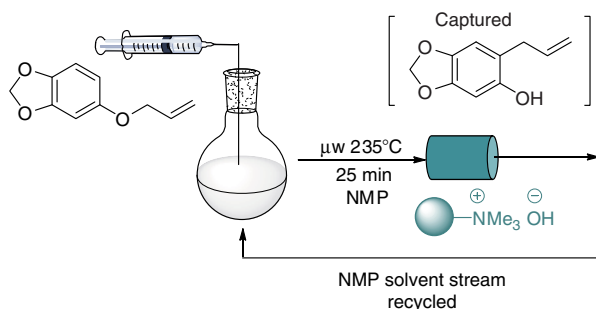
Toluene is also a weakly microwave-absorbing solvent ( $\epsilon' = 2.4$ ,  $\delta = 0.40$ ,  $\epsilon'' = 0.096$ )<sup>[18]</sup> but ideal for many thermal transformations such as the Diels–Alder reaction, which benefits in the transition state from low-polarity solvents. We therefore wished to explore the use of the continuous microwave reactor in the formation of the substituted cyclohexanone depicted in Scheme 7, an intermediate en route to the natural product epibatidine.<sup>[19]</sup> A combined 0.45 M solution of the diene and dienophile in toluene was pumped through the reactor at  $70 \mu\text{L min}^{-1}$ , giving a mean residence time of 36 min. Again, the C/PTFE insert was utilized to allow the desired temperature of 140°C to be maintained (note: this was not possible with the Teflon insert even at the maximum power setting). The exiting

flow stream was then passed through a QP-SA workup cartridge, which promoted decomposition of the intermediate silyl enol and liberation of the desired ketone product. Running the reactor in continuous mode for 80 h afforded ~38 g of the product by processing 336 mL of reaction solution.

Finally, we concluded our evaluation with a high-temperature Claisen rearrangement aimed at determining the long-term thermal stability of the reactor, fittings, and fixtures. We selected the transformation of 5-(allyloxy)benzo[*d*][1,3]dioxole at 225°C in 1-methyl-2-pyrrolidinone (NMP) as the solvent.<sup>[20]</sup> A recycling flow stream was set up allowing the NMP solvent to be reused (Scheme 8).

A 1 M stock solution (50 mL) of the substrate was prepared and pumped through the reactor at a flow rate of 0.1 mL min<sup>-1</sup>, giving a residence time of 25 min. After passing through the reactor, the rearranged phenolic material was captured on an ion-exchange resin (IRA-400 OH form, 3 mmol g<sup>-1</sup>, 1.5 equiv. compared with total material processed), allowing its removal from the flow stream. Unreacted material was automatically routed for recycling by a return feed to the dispensing flask. A syringe pump was used to constantly dispense fresh allyl ether starting material (10 M in NMP, 50-mL syringe) into the starting material dispensing flask (0.6 mL h<sup>-1</sup>) to maintain the approximate initial substrate concentration (1 M). The delivery flask was placed on a magnetic stirrer plate and stirred to ensure rapid mixing and a homogeneous solution. The reactor was run at 225°C for a total of 4 days (96 h; the syringe pump was stopped after 83 h), without any complications or signs of degradation or weakening of the C/PTFE insert or other components. The return feed pipe from the reactor was then set to waste and the system run for a further 16 h, processing the majority of the remaining solution in the delivery flask. The reactor heating was then stopped and the input feed line solution was exchanged for neat THF (7 mL min<sup>-1</sup>, 1 h) to flush the reactor and wash the sequestering ion-exchange column.

Next, the reactor output was adjusted to collect the flow stream and a 1% TFA in MeOH (v/v) solution was used to



**Scheme 8.** Extended processing of a Claisen rearrangement reaction.

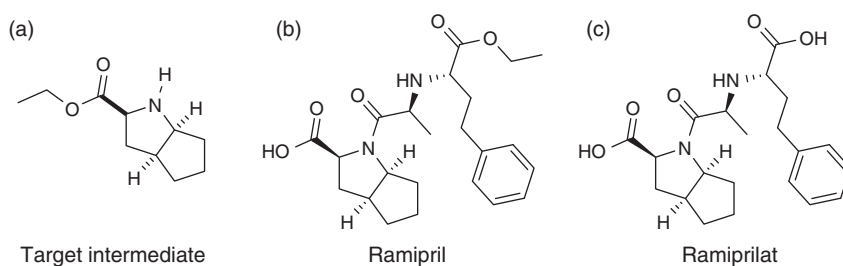


**Fig. 8.** (a) Key building block of ramipril; (b) ramipril; and (c) active metabolite ramiprilat.

release the Claisen rearrangement phenolic product from the scavenging resin (5 mL min<sup>-1</sup>, 2 h). The product obtained (86 g, 88%) was determined to be highly pure (>95% by LC-MS and <sup>1</sup>H NMR) following only simple evaporation of the solvent. This approach as well as reducing the amount of NMP solvent required for the overall process also greatly facilitated the workup process by avoiding the need to separate the product from the high-boiling-point solvent.

### Flow Synthesis of Ramipril Precursor

Having validated the use of the flow cell in the microwave reactor on a series of test reactions, we next turned our attention to the preparation of the bicyclic pyrrolidine ethyloctahydrocyclopentapyrrole-2-carboxylate (Fig. 8a), a key intermediate in the synthesis of the active pharmaceutical ingredient (API) ramipril (Fig. 8b). Ramipril ((2*S*,3*S*,6*S*)-1-[(2*S*)-2-[[[(2*S*)-1-ethoxy-1-oxo-4-phenylbutan-2-yl]amino]-propanoyl]-octahydrocyclopentapyrrole-2-carboxylic acid) is a prodrug; the active metabolite is ramiprilat (Fig. 8c), activated by esterase enzymes in the liver; it is prescribed for the treatment of hypertension and congestive heart failure, acting as an angiotensin-converting enzyme (ACE) inhibitor.<sup>[21]</sup> We were interested in the synthesis of this molecule as part of an investigation into the metabolic stability of the prodrug and so consequently required the preparation of large quantities for appraisal.

The first step of the proposed sequence consists of a condensation reaction between cyclopentanone and benzylamine to give the corresponding imine (Scheme 9). Initial reaction optimization was performed under batch conditions using parallel block reactors. It was shown that the solvent plays an important role; in solvents such as THF or EtOH, the reaction is very slow, whereas in MeCN, it works very efficiently. Therefore, using MeCN and an excess of cyclopentanone (1.4 equiv.) in the presence of MgSO<sub>4</sub>, the imine can be obtained in high purity and yield (87% isolated, >95% conversion) in 30 min. The imine was then directly converted into the pyrrole adduct by reaction with ethyl 3-bromopyruvate (Scheme 9). This was initially conducted as a sequential one-pot process using the previously generated imine solution following only removal of the solid MgSO<sub>4</sub> by filtration. Unfortunately, an approximately 1:1 ratio of regioisomers (Scheme 10) was generated in low overall conversion when 1 equivalent of the  $\alpha$ -bromo carbonyl and 2 equivalents of K<sub>2</sub>CO<sub>3</sub> were added and the reaction mixture heated for 1 h at 85°C (Fig. 9 gives an example LC-MS trace).

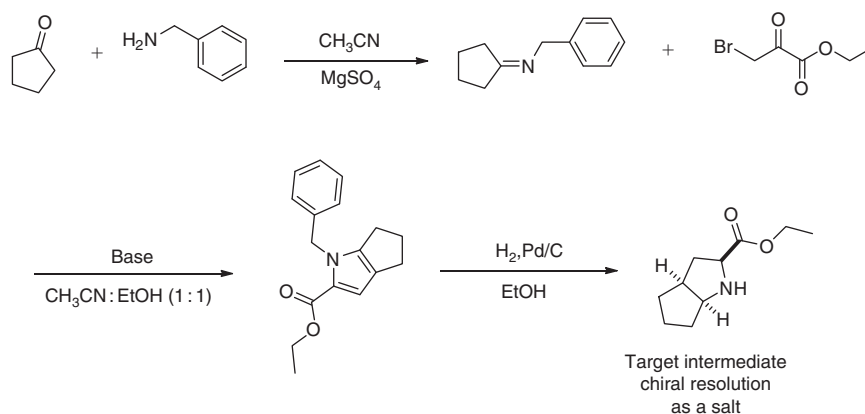
Indeed, the regioselectivity of the process and extent of reaction proved very sensitive to the exact processing conditions; the solvent and especially the base used in the transformation were critical. We therefore isolated the imine and performed a series of optimization experiments that revealed



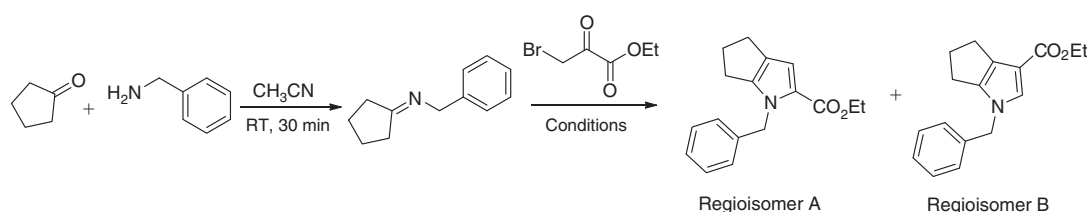
some interesting dependencies (Table 1). From the data, a few general trends can be identified, such as the use of a protic solvent like EtOH or MeOH gives a better overall conversion. At lower temperatures, the preference is for formation of the desired regioisomer A although this is a slow process, whereas at elevated temperatures, the undesired regioisomer B is preferentially formed. Soluble bases such as *N,N*-diisopropylethylamine (DIPEA), Et<sub>3</sub>N and tetrabutylammonium acetate (TBAAc) were more effective for maintaining a fully homogeneous solution, leading to cleaner transformations. The best conditions for performing the reaction were determined to be TBAAc as the base in a 1 : 1 (v/v) mixture of CH<sub>3</sub>CN/EtOH.

The reaction was then transferred to the flow microwave system. Two different reagent input streams were used. The first solution stream contained the benzylamine with cyclopentanone (3 equiv.), MgSO<sub>4</sub> (2 equiv.) and TBAAc (1 equiv.) in MeCN (this pre-reacts, forming the imine in situ). An in-line filter was used to selectively feed the solution in while retaining

the MgSO<sub>4</sub> in the flask. In the second stream was the ethyl bromopyruvate (1 equiv.) in neat EtOH (note: the base is placed in the first solution to prevent it reacting with the ethyl bromopyruvate). Both solutions were then independently pumped at 0.5 mL min<sup>-1</sup> to unite and mix in a standard T-piece. The combined reaction mixture was then passed through the flow microwave, which was heated at 120°C (C/PTFE insert). The exiting solution was purified by solid-phase scavenging using a mixed-bed column comprising a 1:1 mixture of Amberlyst 15 and 21 resins. Direct evaporation of the solvent then allowed isolation of the pyrrole as a pale yellow oil (darkens to brown on standing) in high purity and good yield (Scheme 11). Under these conditions, a 9.3 : 1 ratio of regioisomers A and B was isolated in 77% overall yield on a small scale. Comparable yields of 75 and 78% were achieved on scaling up (×10 and ×40). In each case, the minor regioisomer could be readily removed by column chromatography, but was carried through the next step and removed via recrystallization in the resolution step.



**Scheme 9.** Synthetic pathway to ethyloctahydrocyclopentapyrrole-2-carboxylate.



**Scheme 10.** Regioisomeric mixture from the condensation reaction of cyclopentanone benzyl imine with ethyl 3-bromopyruvate.

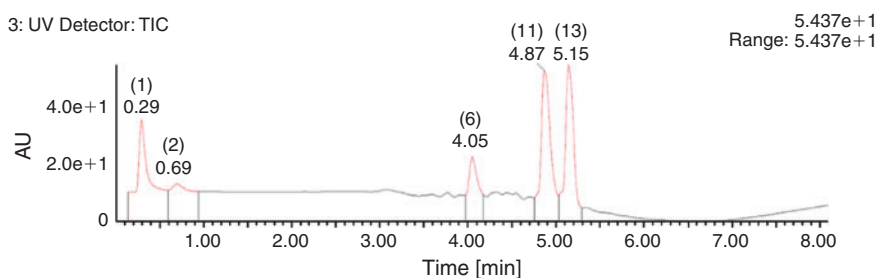


**Fig. 9.** UV trace of the reaction of 3-bromopyruvate and benzylamine imine. The peak at  $R_t = 4.05$  min indicates unreacted imine;  $R_t = 4.87$  min, regioisomer A; and  $R_t = 5.15$  min, regioisomer B.

**Table 1. Optimization of pyrrole formation**  
DIPEA: *N,N*-diisopropylethylamine; rt: room temperature

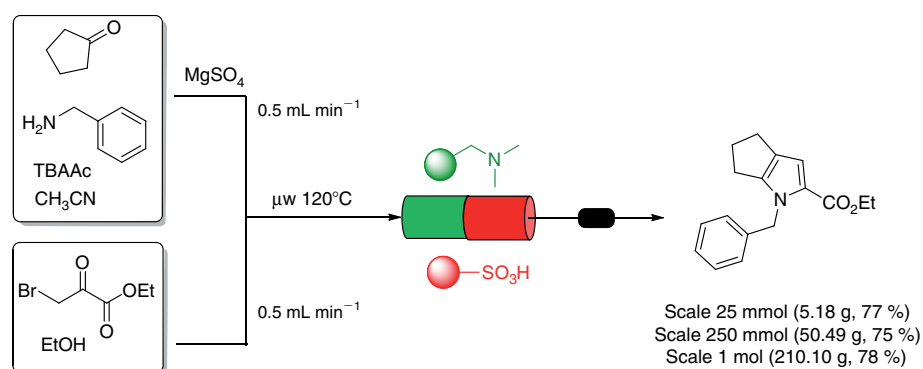
Entry	Conditions				Conversion [%] <sup>A</sup>	
	Solvent	Base	Temperature [°C] <sup>B</sup>	Time [min]	Regioisomer A	Regioisomer B
1	THF	K <sub>2</sub> CO <sub>3</sub>	120	30	11	14
2		DIPEA	120	30	30	7
3		Pyridine <sup>D</sup>	100	30	17	30
4			100	60	31	48
5			120	60	34	50
6	DMF	K <sub>2</sub> CO <sub>3</sub>	100	30	15	28
7		DIPEA	rt	60	23	11
8		DIPEA	60	30	5	20
9		DIPEA	80	30	6	25
10		DIPEA	100	30	8	30
11		DIPEA	120	30	12	45
12		Et <sub>3</sub> N <sup>D</sup>	100	30	9	33
13		Cs <sub>2</sub> CO <sub>3</sub>	100	30	13	30
14		NaOAc	100	30	57	17
15	CH <sub>3</sub> CN	K <sub>2</sub> CO <sub>3</sub>	120	30	18	25
16		DIEA	rt	120	6	21
17			120	30	15	46
18	EtOH	Et <sub>3</sub> N <sup>D</sup>	120	30	18	42
19		DIEA	120	30	10	42
20		K <sub>2</sub> CO <sub>3</sub>	rt	120	62	17
21			60	30	36	36
22			120	30	59	15
23			120	5	27	35
24 <sup>C</sup>			120	5	15	45
25		Bu <sub>4</sub> NCO <sub>3</sub>	120	5	68	15
26		No base	rt	30	25	7
27			100	30	53	28
28			120	30	40	34
29	MeOH	DIPEA	100	30	9	36
30			120	30	15	40
31	CH <sub>3</sub> CN/EtOH	Bu <sub>4</sub> NCO <sub>3</sub>	rt	30	73	4
32			120	5	71	13
33	CH <sub>3</sub> CN		120	5	66	16
34	CH <sub>3</sub> CN/EtOH	Bu <sub>4</sub> NOAc	120	5	83	6
35	CH <sub>3</sub> CN		120	5	50	25
36	EtOH		120	5	58	14

<sup>A</sup>Conversion determined by LC-MS calibrated against <sup>1</sup>H NMR.

<sup>B</sup>Microwave heating.

<sup>C</sup>2 equiv. of ethyl 3-bromopiruvate.

<sup>D</sup>Multiple side products detected.

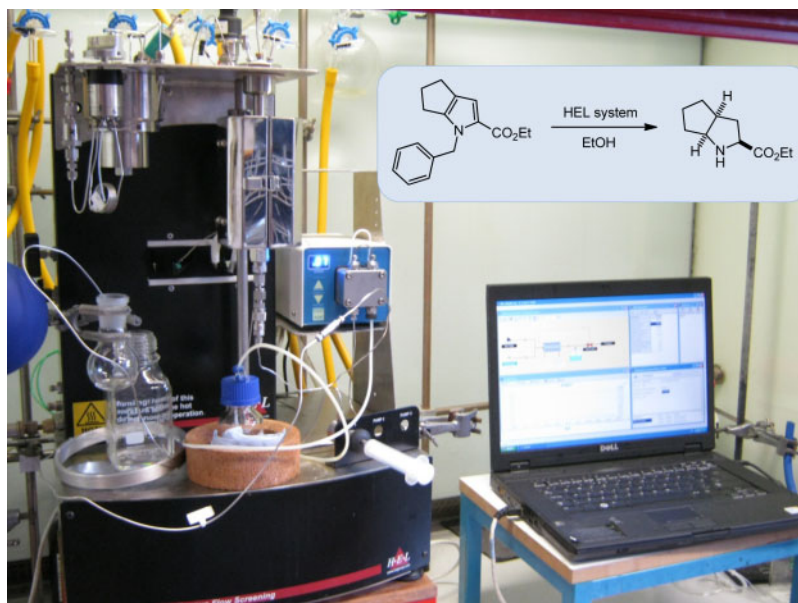


**Scheme 11.** Flow microwave reaction for pyrrole synthesis.

## Hydrogenation

The next step was the reduction of the pyrrole product, removing the benzyl group and simultaneously hydrogenating the aromatic ring to the corresponding pyrrolidine.<sup>[22]</sup> To

accomplish these transformations, we utilized the HEL flow hydrogenation system<sup>[23,24]</sup> (Scheme 12). The flow reactor cartridge was packed (3-cm depth) with Pd/C (10%) using a Johnson Matthey catalyst (Type 10R39), a powder paste



**Scheme 12.** Saturation of the pyrrole cyclization product using HEL hydrogenation reactor.

preparation, which was mixed in a 1 : 1 (w/w) ratio with glass beads<sup>[25]</sup> of dimensions 150–212  $\mu\text{m}$ . This material was loaded by layering the catalyst onto a further 1-cm thick bed of glass beads<sup>[25]</sup> (212–300  $\mu\text{m}$ ) placed at the bottom of the trickle bed column reactor. A rapid optimization starting from previously identified literature conditions identified that a hydrogen pressure of 50 bar at 55°C with a 0.2 M 50 : 1 (v/v) mixture of EtOH/H<sub>2</sub>SO<sub>4</sub> at a flow rate of 1.25 mL min<sup>-1</sup> was ideal for the full conversion of the substrate.

Employing these conditions, the crude racemic pyrrolidine could be easily isolated following evaporation of the solvent, neutralization and re-extraction into EtOAc (quantitative conversion and 97% isolated yield). During the course of this project, over 265 g (5 L, 0.2 M solution) of the starting pyrrole was processed through the reactor in five identical runs of 14-h duration each (total processing time including washing cycles was 72 h). Of particular interest was that the same catalyst bed (described above) was utilized for all five reductions, displaying excellent stability and processing consistency. Indeed, the entire route proved highly reliable, instilling high confidence that this process could be used to reliably and regularly generate this core building block for the synthesis of ramipril. Consequently, we will report in full in the near future the entire synthetic route to the pharmaceutical ingredient ramipril.

## Conclusion

In conclusion, we have demonstrated the application of a modified microwave reactor comprising a flow-through reactor insert for performing microwave-assisted reactions in a series of different chemistries. Several reaction chamber revisions were tested to enhance the flow pathway through the system and create a consistent flow regime leading to predictable reaction profiles. In addition, a carbon-impregnated reactor variation was devised to aid the heating of poorly absorbing solvents, thereby expanding the range of available processing conditions in the device. This simple yet effective solution enabled the various reaction classes to be readily scaled up and should assist in the further development of this industrially important area.

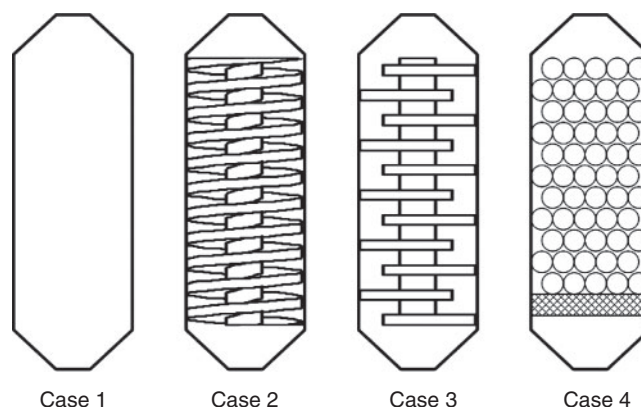


**Fig. 10.** Basic designs of the microwave reactor inserts.

## Experimental

The different reactor cavity designs are described below. Case 1 (Fig. 10) represents the empty cavity with the following dimensions: inner diameter of the glass cylinder  $D = 15.0$  mm; inlet and outlet bores at top and bottom diameter  $d = 1.9$  mm; distance between them  $L = 59.0$  mm; length of the cylindrical section of the reactor cavity  $l = 53.8$  mm (see Fig. 2). Two different Teflon inserts were designed, a helical screw-type insert (case 2, Fig. 10) and a serpentine baffle type insert (case 3, Fig. 10). The exact dimension of these two microwave inserts can be found in the technical drawings (Fig. 11). Case 4 (Fig. 10) is the bead-packed variant of this system. The glass beads of the fixed bed have a diameter  $d_{\text{bead}} = 2.0$  mm. The bed sits on a frit made from fused silica (porosity = 60%), which is situated at the lower end of the cylindrical section of the reactor cavity, directly above the conical end section. The frit height  $h_{\text{frit}}$  is 3.0 mm.

### Experimental Data

All compounds prepared in the testing of the microwave reactor are literature-reported materials. The compounds prepared match the experimental data in the literature.

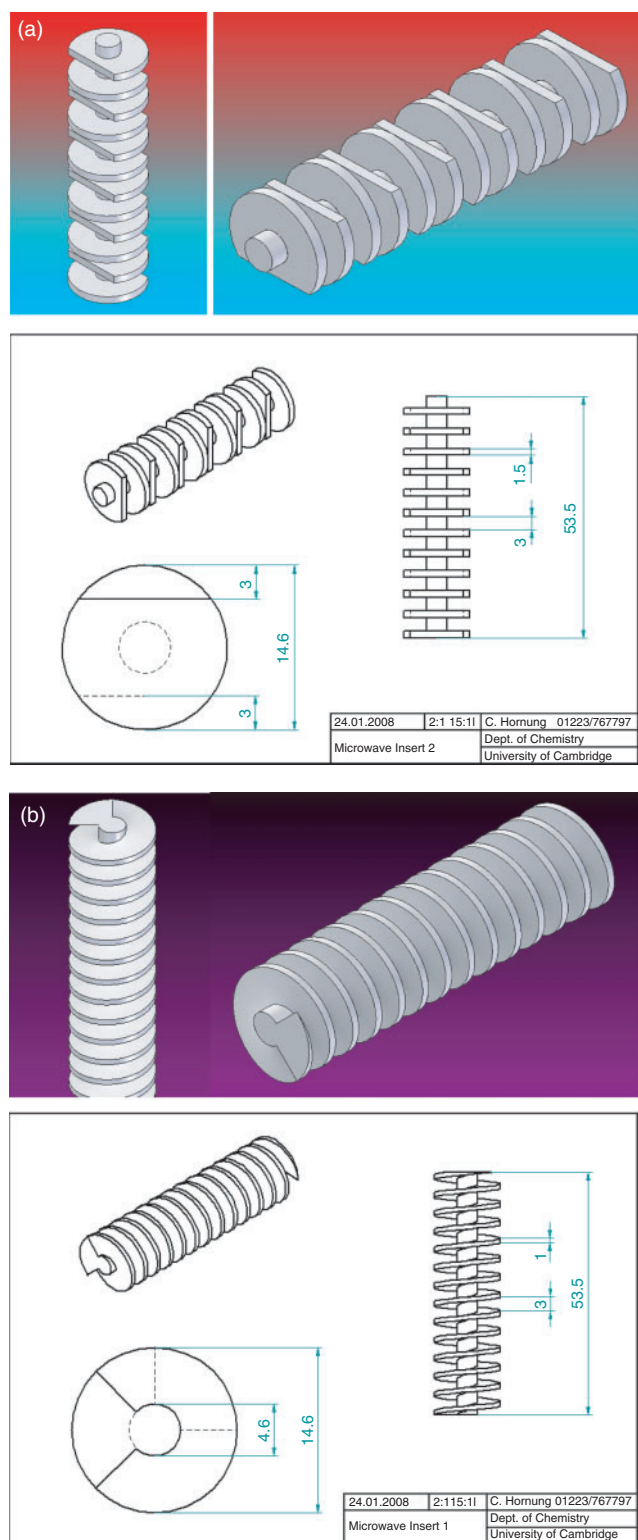


**Fig. 11.** Microwave reactor flow-tube inserts. (a) Top: stepped baffled reactor design; (b) bottom: helical channel (because of the softness of Teflon, the helical insert could not be manufactured to the desired dimensions; the inner diameter was turned down to 9 mm instead of 4.6 mm as shown in the drawing).

#### Synthesis of Cyclopentanone Benzylimine

A mixture of cyclopentanone (2.47 mL, 28 mmol), benzylamine (2.18 mL, 20 mmol) and  $\text{MgSO}_4$  (2.4 g, 20 mmol) in  $\text{CH}_3\text{CN}$  (30 mL) was stirred at room temperature for 30 min.

The  $\text{MgSO}_4$  was filtered off and the solvent evaporated to yield a yellow oil (3 g, 87%).  $\delta_{\text{H}}$  ( $\text{CDCl}_3$ ) 1.77 (t, 2H,  $J$  6.6, H-4 or H-3), 1.86 (t, 2H,  $J$  6.6, H-4 or H-3), 2.28 (t, 2H,  $J$  6.6, H-2 or H-5), 2.41 (t, 2H,  $J$  6.6, H-2 or H-5), 4.44 (s, 2H,  $\text{CH}_2\text{N}$ ), 7.33 (m, 5H, Ph H).  $\delta_{\text{C}}$  ( $\text{CDCl}_3$ ) 25.8 (C-3 or C-4), 26.7 (C-3 or C-4), 27.5 (C-2 or C-5), 28.8 (C-2 or C-5), 53.8 ( $\text{CH}_2\text{N}$ ), 126.2 (*p*-C Ph), 127.5, 128.1 (*o*-C Ph), 140.6 (C-1 Ph), 173.1 (C=N).  $m/z$  (electrospray ionization-high resolution mass spectrometry (ESI-HRMS)) Calc. for  $\text{C}_{12}\text{H}_{15}\text{N}$ . 173.1204. Found: 173.1202.

#### Synthesis of Ethyl 1-Benzyl-1,4,5,6-tetrahydrocyclopenta[b]pyrrole-2-carboxylate in Batch

Cyclopentanone benzylimine (0.86 g, 5 mmol), ethyl 3-bromopyruvate (0.65 mL, 5 mmol) and TBAAC (750 mg, 2.5 mmol) in 1:1  $\text{CH}_3\text{CN}/\text{EtOH}$  (10 mL) were heated in a Biotage Emrys Initiator reactor at  $120^\circ\text{C}$  for 5 min. After scavenging with 1:1 Amberlyst 15/Amberlyst 21 (A-15/A-21) for 30 min, filtration and evaporation of the solvent gave a yellow oil consisting of a 9.3:1 mixture of isomers A and B (941 mg, 70%).

#### Synthesis of Ethyl 1-Benzyl-1,4,5,6-tetrahydrocyclopenta[b]pyrrole-2-carboxylate in Flow

A solution of cyclopentanone (6.63 mL, 75 mmol), benzylamine (2.72 mL, 25 mmol),  $\text{MgSO}_4$  (3 g, 25 mmol), and TBAAC (3.8 g, 12.5 mmol) in  $\text{CH}_3\text{CN}$  (made up to 25 mL) was pumped from the R2 flow system at a flow rate of  $0.5 \text{ mL min}^{-1}$ . At the same time, ethyl bromopyruvate (3.25 mL, 25 mmol) in EtOH (made up to 25 mL) was pumped at the same flow rate. Both solutions were mixed in a T-piece, and the combined flow stream ( $1.0 \text{ mL min}^{-1}$ ) was passed through the microwave reactor, which was maintained at  $120^\circ\text{C}$ . Purification with a column of 1:1 A-15/A-21 yielded the *title compound* as a yellow oil (5.2 g, 77%) in a 9.3:1 mixture of isomers A and B.

**Regioisomer A.** Pale yellow oil.  $\delta_{\text{H}}$  ( $\text{CDCl}_3$ ) 1.29 (t, 3H,  $J$  7.1,  $\text{CH}_3$ ), 2.39 (q, 2H,  $J$  7.1,  $\text{CH}_2\text{-CH}_2\text{-CH}_2$ ), 2.63 (dt, 4H,  $J$  7.3 and 7.2,  $\text{CH}_2\text{-CH}_2\text{-CH}_2$ ), 4.23 (c, 2H,  $J$  7.1,  $\text{CH}_2\text{CH}_3$ ), 5.51 (s, 2H, C- $\text{CH}_2\text{-N}$ ), 6.82 (s, 1H, CH), 7.09 (d, 2H,  $J$  7.3, *o*-H Ph), 7.23 (t, 1H,  $J$  7.2, *p*-H Ph), 7.3 (t, 2H,  $J$  7.3, *m*-H Ph).  $\delta_{\text{C}}$  ( $\text{CDCl}_3$ ) 14.4 ( $\text{CH}_3$ ), 24.8, 24.9 ( $\text{CH}_2\text{-CH}_2\text{-CH}_2$ ), 28.5 ( $\text{CH}_2\text{-CH}_2\text{-CH}_2$ ), 50.2 (C- $\text{CH}_2\text{-N}$ ), 59.3 ( $\text{CH}_2\text{-CH}_3$ ), 112.8 (C-CH-N), 126.5 (*o*-C Ph), 127 (*p*-C Ph), 128.4 (*m*-C Ph), 124.5, 126.5, 138.5, 147.2, 161.2 (C quat.).  $m/z$  (ESI-HRMS) Calc. for  $\text{C}_{17}\text{H}_{20}\text{NO}_2$  270.1494. Found 270.1502.

**Regioisomer B.** Pale yellow oil.  $\delta_{\text{H}}$  ( $\text{CDCl}_3$ ) 1.32 (t, 3H,  $J$  7.1,  $\text{CH}_3$ ), 2.38 (q, 2H,  $J$  7.1,  $\text{CH}_2\text{-CH}_2\text{-CH}_2$ ), 2.51 (t, 2H,  $J$  7.2,  $\text{CH}_2\text{-CH}_2\text{-CH}_2$ ), 2.80 (t, 2H,  $J$  6.9,  $\text{CH}_2\text{-CH}_2\text{-CH}_2$ ), 4.24 (q, t, 2H,  $J$  7.1,  $\text{CH}_2\text{CH}_3$ ), 4.94 (s, 2H, C- $\text{CH}_2\text{-N}$ ), 7.12 (d, 2H,  $J$  7.1, *o*-H Ph), 7.21 (s, 1H, C-CH-N), 7.26–7.35 (m, 3H, *p*-H Ph and *m*-H Ph).  $\delta_{\text{C}}$  ( $\text{CDCl}_3$ ) 14.4 ( $\text{CH}_3$ ), 24.6, 25.9, 28.7 ( $\text{CH}_2\text{-CH}_2\text{-CH}_2$ ), 52.3 (C- $\text{CH}_2\text{-N}$ ), 59.3 ( $\text{CH}_2\text{-CH}_3$ ), 111.2 (C-CH-N), 127.1 (*o*-C Ph), 127.8 (*p*-C Ph), 128.7 (*m*-C Ph), 128.3, 128.4, 136.8, 138.9, 165.2 (C quat.).  $m/z$  (ESI-HRMS) Calc. for  $\text{C}_{17}\text{H}_{20}\text{NO}_2$  270.1494. Found: 270.1505.

#### Ethyl Octahydrocyclopenta[b]pyrrole-2-carboxylate.<sup>[22]</sup>

Following reduction, the major regioisomer was isolated in 62% yield by recrystallization of the crude material from EtOAc.  $\delta_{\text{H}}$  ( $\text{CDCl}_3$ ) 4.18 (q, 2H,  $J$  7.6,  $\text{OCH}_2$ ), 3.65 (m, 1H, Cl-H), 3.55 (dd, 1H,  $J$  10 and 6.2, C-3-H), 2.59 (m, 2H, C-5-H), 2.34 (m, C-4-H), 1.88 (br. s, 1H, NH), 1.34–1.72 (m, 7H,  $3 \times \text{CH}_2$  and C-4-H), 1.25 (t, 3H,  $J$  7.6,  $\text{CH}_3$ ).  $m/z$  (ESI-HRMS) Calc. for  $\text{C}_{17}\text{H}_{20}\text{NO}_2$  183.1259. Found: 183.1268.

## Acknowledgements

We gratefully acknowledge financial support from the Royal Society (to IRB) and the BP Endowment (to SVL), and from Biotage AG for the kind loan of the microwave equipment.

## References

- [1] (a) P. Lidström, J. P. Tierney, B. Wathey, J. Westman, *Tetrahedron* **2001**, *57*, 9225. doi:10.1016/S0040-4020(01)00906-1  
 (b) C. O. Kappe, A. Stadler, *Microwaves in Organic and Medicinal Chemistry* **2005** (Wiley-VCH: Weinheim).  
 (c) J. P. Tierney, P. Lidström (Eds), *Microwave-assisted Organic Synthesis* **2005** (Blackwell Publishing Ltd: Oxford).
- [2] (a) V. Hessel, *Chem. Eng. Technol.* **2009**, *32*, 1655. doi:10.1002/CEAT.200900474  
 (b) M. Baumann, I. R. Baxendale, S. V. Ley, *Mol. Divers.* **2011**, *15*, 613. doi:10.1007/S11030-010-9282-1  
 (c) A. Sachse, A. Galarneau, B. Coq, F. Fajula, *New J. Chem.* **2011**, *35*, 259. doi:10.1039/C0NJ00965B
- [3] (a) L. F. Raveglia, G. A. M. Giardina, *Future Med. Chem.* **2009**, *1*, 1019.  
 (b) W. G. Devine, N. E. Leadbeater, *ARKIVOC* **2011**, *V*, 127.  
 (c) S. V. Ley, I. R. Baxendale, in *Systems Chemistry* (Eds M. G. Hicks, C. Kettner) **2009**, Proceedings of the Beilstein-Institut Workshop, 26–30 May, 2008, Bozen, Italy, 65–85. Available at <http://www.beilsteininstitut.de/Bozen2008/Proceedings/Ley/Ley.pdf>  
 (d) K. Geyer, P. H. Seeberger, in *Systems Chemistry* (Eds M. G. Hicks, C. Kettner) **2009**, Proceedings of the Beilstein-Institut Workshop, 26–30 May, 2008, Bozen, Italy, 87–107. Available at <http://www.beilstein-institut.de/Bozen2008/Proceedings/Seeberger/Seeberger.pdf>  
 (e) S. V. Ley, I. R. Baxendale, *Chimia* **2008**, *62*, 162. doi:10.2533/CHIMIA.2008.162
- [4] (a) I. R. Baxendale, M. R. Pitts, *Chimica Oggi, Chemistry Today* **2006**, *24*, 241.  
 (b) I. R. Baxendale, J. J. Hayward, S. V. Ley, *Comb. Chem. High Throughput Screen.* **2007**, *10*, 802. doi:10.2174/138620707783220374  
 (c) T. N. Glasnov, C. O. Kappe, *Macromol. Rapid Commun.* **2007**, *28*, 395. doi:10.1002/MARC.200600665  
 (d) J. R. Schmink, C. M. Kormos, W. G. Devine, N. E. Leadbeater, *Org. Process Res. Dev.* **2010**, *14*, 205. doi:10.1021/OP900287J  
 (e) T. N. Glasnov, C. O. Kappe, *Chem. – Eur. J.* **2011**, *17*, 11956. doi:10.1002/CHEM.201102065
- [5] (a) S. Saaby, I. R. Baxendale, S. V. Ley, *Org. Biomol. Chem.* **2005**, *3*, 3365. doi:10.1039/B509540A  
 (b) I. R. Baxendale, J. Deeley, C. M. Griffiths-Jones, S. V. Ley, S. Saaby, G. K. Tranmer, *Chem. – Eur. J.* **2006**, *12*, 4407. doi:10.1002/CHEM.200501400  
 (c) C. J. Smith, J. Iglesias-Sigüenza, I. R. Baxendale, S. V. Ley, *Org. Biomol. Chem.* **2007**, *5*, 2758. doi:10.1039/B709043A  
 (d) J. Sedelmeier, S. V. Ley, H. Lange, I. R. Baxendale, *Eur. J. Org. Chem.* **2009**, 4412. doi:10.1002/EJOC.200900344
- [6] M. C. Bagley, R. L. Jenkins, M. C. Lubinu, C. Mason, R. Wood, *J. Org. Chem.* **2005**, *70*, 7003. doi:10.1021/JO0510235
- [7] A. Debache, R. Boulcina, A. Belfaitah, S. Rhouati, B. Carboni, *Synlett* **2008**, *2008*, 509. doi:10.1055/S-2008-1032093
- [8] See [http://www.uniqsis.com/paProductsDetail.aspx?ID=ACC\\_MIX](http://www.uniqsis.com/paProductsDetail.aspx?ID=ACC_MIX) for details on the baffled mixer chip (verified September 2012).
- [9] (a) H. R. Sahoo, J. G. Kralj, K. F. Jensen, *Angew. Chem. Int. Ed.* **2007**, *46*, 5704. doi:10.1002/ANIE.200701434  
 (b) J. Wiss, C. Fleury, C. Heuberger, U. Onken, M. Glor, *Org. Process Res. Dev.* **2007**, *11*, 1096. doi:10.1021/OP7000645  
 (c) K. Yamatsugu, S. Kamijo, Y. Suto, M. Kanai, M. Shibasaki, *Tetrahedron Lett.* **2007**, *48*, 1403. doi:10.1016/J.TETLET.2006.12.093  
 (d) H. Lebel, O. Leogane, *Org. Lett.* **2006**, *8*, 5717. doi:10.1021/OL0622920  
 (e) M. Baumann, I. R. Baxendale, S. V. Ley, N. Nikbin, C. D. Smith, J. P. Tierney, *Org. Biomol. Chem.* **2008**, *6*, 1577. doi:10.1039/B801631N  
 (f) M. Baumann, I. R. Baxendale, S. V. Ley, N. Nikbin, C. D. Smith, *Org. Biomol. Chem.* **2008**, *6*, 1587. doi:10.1039/B801634H
- [10] (a) For selected examples, see: V. Singh, S. Kaur, V. Sapehiyi, J. Singh, G. L. Kad, *Catal. Commun.* **2005**, *6*, 57. doi:10.1016/J.CATCOM.2004.10.011  
 (b) M. S. Manhas, S. N. Ganguly, S. Mukherjee, A. K. Jain, A. K. Bose, *Tetrahedron Lett.* **2006**, *47*, 2423. doi:10.1016/J.TETLET.2006.01.147  
 (c) B. Tyagi, M. K. Mishra, R. V. Jasra, *J. Mol. Catal. A – Chem.* **2007**, *276*, 47. doi:10.1016/J.MOLCATA.2007.06.003  
 (d) Y. Reddy, S. Thirupathi, S. Vijayakumar, P. Crooks, P. Dasari, P. Reddy, P. Narsimha, B. Rajitha, *Synthetic Commun.* **2008**, *38*, 2082. doi:10.1080/00397910802209091  
 (e) A. Sinhamahapatra, N. Sutradhar, S. Pahari, H. C. Bajaj, A. B. Panda, *Appl. Catal. A – Gen.* **2011**, *394*, 93. doi:10.1016/J.APCATA.2010.12.027  
 (f) Q. Zhang, S. Zhang, Y. Deng, *Green Chem.* **2011**, *13*, 2619. doi:10.1039/C1GC15334J  
 (g) J. Zak, D. Ron, E. Riva, H. P. Harding, B. C. S. Cross, I. R. Baxendale, *Chem. – Eur. J.* **2012**, *18*, 9901. doi:10.1002/CHEM.201201039
- [11] (a) S. V. Ley, A. G. Leach, R. I. Storer, *J. Chem. Soc., Perkin Trans. 1* **2001**, 358. doi:10.1039/B008814P  
 (b) R. Martínez-Palou, *J. Mex. Chem. Soc.* **2007**, *51*, 252.  
 (c) N. E. Leadbeater, H. M. Torenus, in *Microwaves in Organic Synthesis* (Ed. A. Loupy) **2008**, Ch. 7, pp. 327–361 (Wiley-VCH: Weinheim).
- [12] Weflon is Milestone's proprietary microwave absorbing carbonm-pregnated Teflon material; Si/C, see: D. Obermayer, B. Gutmann, C. O. Kappe, *Angew. Chem. Int. Ed.* **2009**, *48*, 8321. doi:10.1002/ANIE.200904185
- [13] (a) G. E. Keck, J. B. Yates, *J. Am. Chem. Soc.* **1982**, *104*, 5829. doi:10.1021/JA00385A066  
 (b) S. D. Burke, W. F. Fobare, D. M. Armistead, *J. Org. Chem.* **1982**, *47*, 3348. doi:10.1021/JO00138A037  
 (c) F. Le Guyader, B. Quiclet-Sire, S. Seguin, S. Z. Zard, *J. Am. Chem. Soc.* **1997**, *119*, 7410. doi:10.1021/JA9708878
- [14] P.-J. Shim, H.-D. Kim, *Tetrahedron Lett.* **1998**, *39*, 9517. doi:10.1016/S0040-4039(98)02228-X
- [15] (a) T. L. Mindt, R. Schibli, *J. Org. Chem.* **2007**, *72*, 10247. doi:10.1021/JO702030E  
 (b) H. Harkat, A. Y. Dembelé, J.-M. Weibel, A. Blanc, P. Pale, *Tetrahedron* **2009**, *65*, 1871. doi:10.1016/J.TET.2008.10.112  
 (c) J. Alemán, V. del Solar, L. Cubo, A. G. Quiroga, C. N. Ranninger, *Dalton Trans.* **2010**, 10601. doi:10.1039/C0DT00506A
- [16] G. Sun, C. Cheng, K. L. Wooley, *Macromolecules* **2007**, *40*, 793. doi:10.1021/MA062592X
- [17] C. R. Sarko, in *Microwave-assisted Organic Synthesis* (Eds J. P. Tierney, P. Lidström) **2005**, Ch. 8, pp. 222–236 (Blackwell Publishing Ltd: Oxford).
- [18] B. L. Hayes, *Microwave Synthesis: Chemistry at the Speed of Light* **2002** (CEM Publishing: Matthews, NC).
- [19] J. Habermann, S. V. Ley, J. S. Scott, *J. Chem. Soc., Perkin Trans. 1* **1999**, *10*, 1253. doi:10.1039/A901802F
- [20] (a) P. F. Schuda, W. A. Price, *J. Org. Chem.* **1987**, *52*, 1972. doi:10.1021/JO00386A014  
 (b) I. R. Baxendale, A.-L. Lee, S. V. Ley, *J. Chem. Soc., Perkin Trans. 1* **2002**, 1850. doi:10.1039/B203388G
- [21] (a) A. S. Zentiva, H. Stepankova, P. Pihera, J. Hajicek, A Method of Preparation of Ramipril, WO patent, 121084, **2005**.  
 (b) V. Teetz, R. Geiger, H. Baul, *Tetrahedron Lett.* **1984**, *25*, 4479. doi:10.1016/S0040-4039(01)81471-4  
 (c) M. Baumann, I. R. Baxendale, S. V. Ley, N. Nikbin, *Beilstein J. Org. Chem.* **2011**, *7*, 442. doi:10.3762/BJOC.7.57
- [22] H. Urbach, X. Uenning, *Tetrahedron* **1985**, *26*, 1839. doi:10.1016/S0040-4039(00)94751-8

- [23] Continuous Flow Catalytic Reactions with FlowCAT. Available at <http://www.helgroup.com/reactor-systems/hydrogenation-catalysis/flowcat-highpressure-flowchemistry-in-a-compact-unit/>
- [24] J. M. Hawkins, Trickle Bed Flow Hydrogenation Using Shallow Beds of Fine Catalyst Particles: Enhanced Diastereoselectivity, Purity Control, and Catalyst Activity Relative to Batch Hydrogenations, Abstracts of Papers, 242nd ACS National Meeting & Exposition, Denver, CO, United States, 28 August–1 September 2011.
- [25] Glass beads acid-washed; 212–300  $\mu\text{m}$  available from Sigma–Aldrich cat. no. G1277 and 150–212  $\mu\text{m}$  available from Sigma–Aldrich cat. no. G1145.